Available online at www.sciencedirect.com
SCIENCE DIRECT®
Nuclear Instruments and Methods in Physics Research A 535 (2004) 115–120
NUCLEAR INSTRUMENTS & METHODS IN PHYSICS RESEARCH Section A
www.elsevier.com/locate/nima

A thin-walled air-ionization chamber for proton therapy

Stanislav I. Potashev[a,*], Sergey V. Akulinichev[a], Yuri M. Burmistrov[a], Mikhail V. Mordovskoy[a], Alexander I. Drachev[b]

[a]*Institute for Nuclear Research (INR), Russian Academy of Sciences, 60th October Anniversary Prospect, 7A, Moscow 117312, Russia*
[b]*Enicolopov Institute of Synthetic Polymer Materials, Moscow, Russia*

Available online 9 August 2004

Abstract

A thin-walled air-ionization chamber with narrow gap was built for monitoring the proton therapy beam at the Moscow linac. The key chamber elements are 1.5 μm thick polyimide films mounted on quartz and stainless steel rings by means of a special technology. Gold-coated films were used as chamber electrodes. Consisting of only a small amount of material, this chamber allows the detection of low-energy protons and nuclei. The 64 cm^2 sensitive area contains 60 strips for measuring two-dimensional dose profiles. The low noise as well as the 2 mm gap between the electrodes allow to reach a sensitivity of 1 pA for protons and electrons. No ageing effects were observed after about 10^{17} protons had passed through the chambers.
© 2004 Elsevier B.V. All rights reserved.

PACS: 87.53.Qc; 29.40.−n; 29.40.Gx

Keywords: Proton therapy; Ionization chamber; Thin film

1. Introduction

An accurate measurement of proton beam parameters is very important for the proton therapy which will be carried out in INR at the Moscow linear accelerator. The irradiation quality control requires an accurate monitoring of the main beam parameters. For the case of scanning-beam irradiation techniques used in proton therapy the required basic equipment has been described in earlier papers [1–3]. In particular, ionization chambers are widely used for dosimetry in radiotherapy [4]. However, any material in front of the patient disturbs the incident beam and leads to undesirable irradiation by secondary particles. Therefore the chamber walls must be as thin as possible. Here, we present a thin-walled air-ionization chamber, which provides an accurate measurement of both total energy loss and spatial distribution of incident particles for

*Corresponding author.
E-mail address: potashev@a120.inr.troitsk.ru (S.I. Potashev).

0168-9002/$ - see front matter © 2004 Elsevier B.V. All rights reserved.
doi:10.1016/j.nima.2004.07.116

each beam pulse in real time during a patient's treatment.

2. Detector design and read-out electronics

The design of this detector was developed according to the following requirements: minimum amount of material exposed to the beam; low leakage current in order to achieve high sensitivity; narrow gap in order to avoid significant signal reduction due to ion recombination in the air used as active medium; negligible electrode deflection in high electric fields in order to avoid charge variations.

The whole device is a sandwich of two identical chamber units. The internal structure of each of these chamber units (see Fig. 1) represents an anode located between the multistrip and the continuous cathodes. The electrodes are mounted in a cave-like fluoropolymer structure which provides stable operation and low leakage current. The multistrip cathode consists of 1.5 μm polyimide film mounted on a quartz-glass ring and coated by a 0.15 μm layer of copper and 0.05 μm layer of gold. The key parameters of each chamber unit are given in Table 1. The influence of the chamber on the beam is minimal due to thin chamber windows which serve as cathodes. For example, the neutron flux generated by one

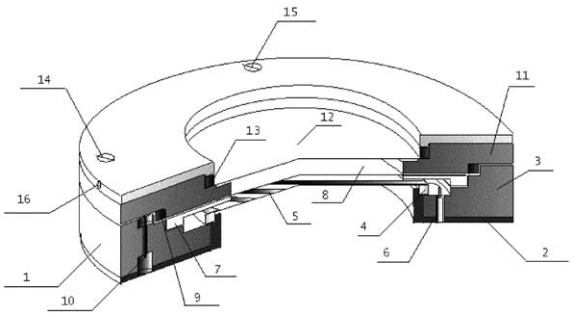

Fig. 1. One of two units of the thin-walled air-ionization chamber. 1—base; 2—screen; 3—insulator; 4—quartz-glass ring; 5—multistrip cathode; 6—multistrip cathode connector; 7—anti-spark tip; 8—anode; 9—large metal ring; 10—anode connector; 11—insulator lid; 12—continuous cathode; 13—small metal ring; 14—metal lid; 15—screw; 16—continuous cathode connector.

Table 1
Detector key parameters

Diameter of active area	90 mm
Distance between anode and cathode	2 mm
Width and number of strips	3 mm × 30 mm
Active medium	Atmospheric air
Cathode window thickness	0.4 mg/cm^2
Anode thickness	0.7 mg/cm^2
Total thickness including air in chamber unit	2.0 mg/cm^2

incident proton in the chamber can be estimated as 10^{-6}. The air between the anode and the two cathodes represents two detection regions. The charge collection efficiency is determined by ion recombination in the chamber air and is expected to be 0.98 at 1000 V high voltage for the 1 nA average incident proton current and the 1/200 accelerator duty cycle at 209 MeV.

The chamber current produced by the ions of a single accelerator spill is digitized by time slices for fine charge reconstruction in the chamber. We measured signals both from the continuous cathodes and from different strips of the opposite cathodes.

The read-out electronics includes the preamplifiers PA and analog multiplexers 4MUX located close to the chamber and the analog/digital signal processor ADSP board installed in a computer. The board contains the sixteen logical output chips LOGOUT, sixteen analog input multiplexers 16MUX, a digital control amplifier DCA, a digital signal processor DSP, an analog-to-digital converter ADC, and a buffer memory BM.

The shape of every pulse induced in the chamber by a single beam spill is registered from each sensitive strip and then the charge is calculated. The measurements are processed by the DSP which evaluates in real time the pulse shape and total beam ionization loss together with their transversal profiles. We have used a fast analog-to-digital converter and analog multiplexers in order to make the electronics compact. The signal registration sequence is defined by the code in the DSP, which switches the multiplexers. The main parameters of the electronics are given in Table 2.

Table 2
Readout electronics: main parameters

PA gain	12 mV/nA
DSP frequency	up to 3 MHz
Frequency per channel in the 62 input mode	up to 45 kHz
ADSP conversion gain	0.31–2.5 mV/dig.ch.

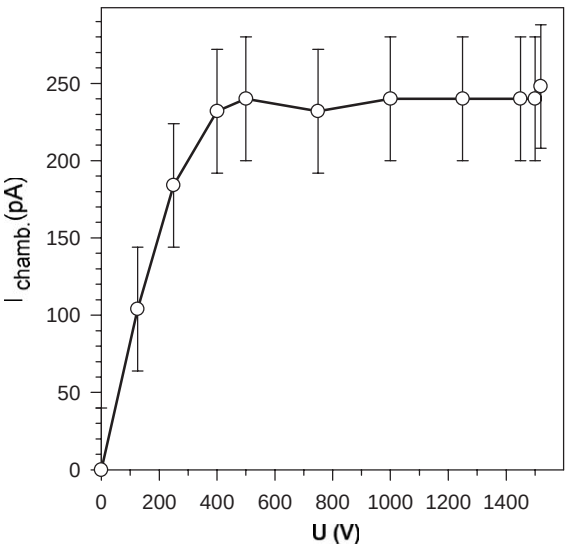

Fig. 2. Total current in the chamber versus applied high voltage. The chamber is irradiated with β-particles from a $^{90}Sr(^{90}Y)$ source.

3. Test with radioactive β-source

First, the chamber was tested using a $^{90}Sr(^{90}Y)$ β-source with a total intensity of $1.8 \times 10^8\ s^{-1}$. Signals from all cathodes were combined together for test purposes and a measurement of the direct current was performed. The dependence of the total current in a chamber unit on the high voltage applied is presented in Fig. 2. The ionization plateau is between 800 and 1500 V. Breakdown was observed above 1520 V but stable operation of the chamber was restored when the high voltage was decreased to below 1500 V.

The measured chamber current at the plateau corresponds to 5 pA equivalent initial electron current or to 2.5 pA initial proton current at 200 MeV.

4. Results of proton beam measurements at 209 MeV

The proton beam at 209 MeV passed through a 1.2 m long collimator with an internal diameter of 30 mm. The accelerator bunch duration was 120 μs and the frequency was 50 Hz. The read-out process was synchronized with the accelerator spill.

Oscillograms from all channels were continuously digitized. Detailed information on the pulse height, rise time and duration of the chamber pulse was obtained at the maximal ADSP frequency of 3 MHz. A typical pulse shape is shown in Fig. 3. Here, the pulse duration was 150 μs and the rise time was 35 μs. The background has the shape of a wave oscillation and can be easily filtered out. No breakdown was registered during the measurements. The sensitivity to the charge measured in the chamber is about 250 fC. Taking into account the fact that at least 28 ion pairs are produced by one proton, the charge sensitivity to the incident

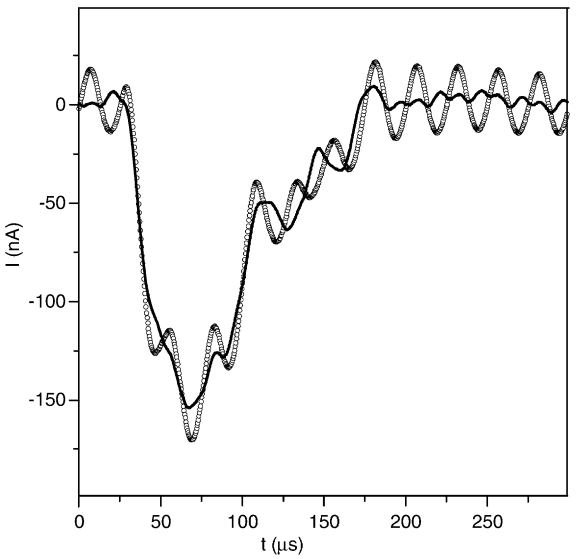

Fig. 3. The pulse shape measured in a single chamber strip. The circles are the original signal induced by a 209 MeV proton beam. The line is the same signal after wave oscillation subtraction.

beam is estimated as 10 fC. Using the readout electronics characteristics, the total charge in the pulse can be estimated as 11 pC. It was produced by the 380-fC charge in the primary beam bunch, taking into account only the energy loss of protons at 209 MeV.

The correlation between signals from a continuous cathode and different strips at 1300 V is shown in Fig. 4. For the actual ion chamber location, the proton beam center crossed the 23rd and 22nd strips. Fig. 4(a) demonstrates a clear correlation between charges collected in the 22nd strip and in the continuous cathode, which served as a monitor. The correlation between charges collected in the continuous cathode and the 16th strip is shown in Fig. 4(b). The 16th strip was located in the vicinity of the beam boundary. Fig. 4(c), finally, illustrates the correlation between charges collected in the continuous cathode and in the 7th strip at the chamber periphery. Here, an obscure pattern is observed because only scattered particles can contribute to the signal. The clearest correlation is obtained between the continuous cathode charge and the combination of charges from the 22nd (70%) and 23rd (30%) cathodes. This is shown in Fig. 4(d), where the correlation is more obvious at low values. The observed patterns are the same at 1000 V and 800 V for a typical intensity of the order of 10^7 protons per spill but they become vague at 600 and 400 V.

The behaviour of the charge response from the continuous cathode and several strips is shown in Fig. 5. In this figure, the mixture of the response from the 22nd and 23rd strips in the proportion 7/3 is also shown. The time instability of the beam intensity and position is the main contribution to the uncertainty of the measured energy loss in the chamber.

The charge collected on the continuous cathode was used as a reference value. We normalized several strip responses to the one of the continuous cathode under the assumption of their linear dependence and we summed the charges over 1-s time intervals. The resulting curves obtained for

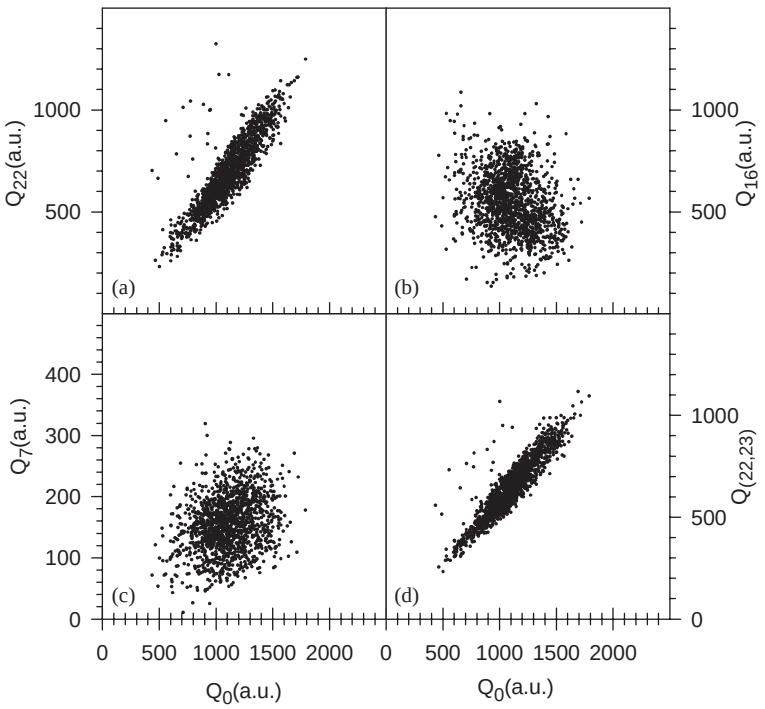

Fig. 4. Correlation between charges (arbitrary units) collected in the continuous cathode and the 22nd strip (a), 16th strip (b), 7th strip (c) and the combination of two strips (0.7 of the 22nd strip and 0.3 of the 23rd strip) (d) at 1300 V.

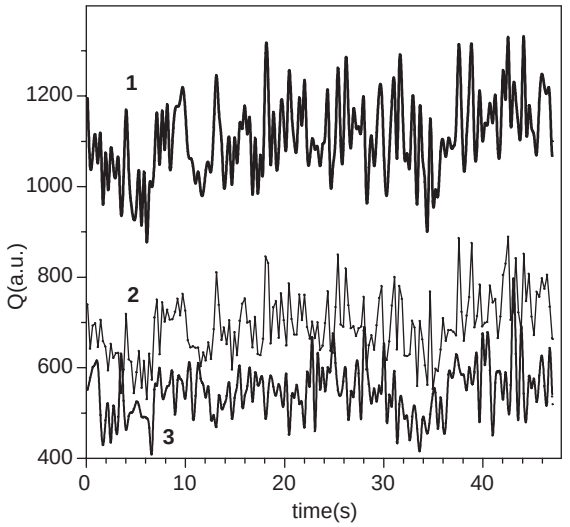

Fig. 5. Charge response (in arbitrary units) from the continuous cathode (1), 22nd strip (2), and 16th strip (3) for 209 MeV protons versus time. The response is induced by 16 beam spills summed at each point. The high voltage applied is 1300 V.

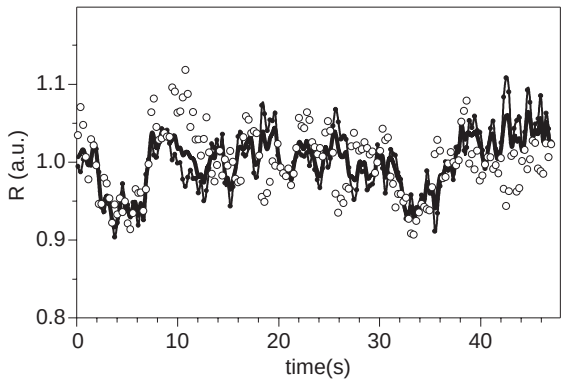

Fig. 6. The normalized ratio R of the response from the 22nd strip (fine line with closed circles), the 23rd strip (open circles) and their combination (as in two previous figures, fat line) versus time. The measurement conditions are the same as in the previous figure. The data are averaged over a 1 s time interval.

the 22nd and the 23rd strip and their combination are almost horizontal (Fig. 6).

Furthermore, measurements were carried out for a 209 MeV proton beam passing through a 200 mm long polystyrene phantom and a plastic wedge of variable thickness. By varying the

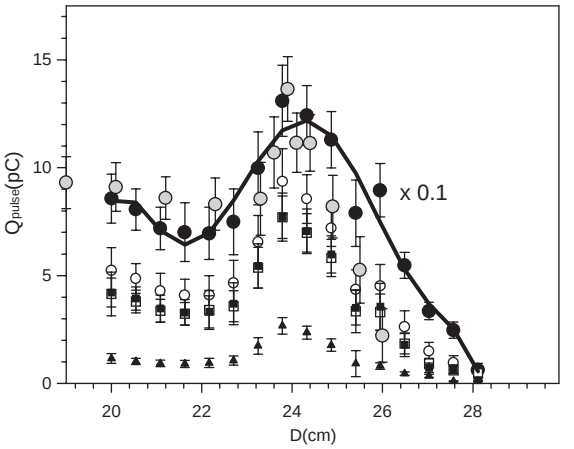

Fig. 7. The dose-depth distribution obtained from data of the 22nd (open circles), 23rd (open rectangles), 16th (closed rectangles), and 7th (closed triangles) strip and the continuous cathode (closed circles, magnitude multiplied by 0.1) and for the signal (in relative units) from a diode dosimeter (grey circles). The curve is a regression.

amount of tissue-equivalent material in front of the chamber, we measured a dose depth distribution at 3×10^5 Hz/mm^2. The Bragg peak observed in these distributions for the continuous cathode and different strips is shown in Fig. 7.

In order to estimate the number of protons and the dose per spill, we measured the mean charge collected in the continuous cathode. This value was approximately 150 pC for a depth of water-equivalent material equal to 24 cm. This corresponds to 5×10^6 protons/spill of initial beam provided that about 175 ion pairs are produced by each proton at the Bragg peak inside the chamber gap. The amount of air in a single chamber gap is equal to 16.4 mg. Thus, we get for the dose delivered in the chamber 0.3 mGy/spill or 1 Gy/min at a beam frequency of 50 Hz.

The thin windows allow to use this chamber as a tracking detector for nuclei at low energy. Results of calculations for ^{12}C penetration through the entrance window at different initial energies are presented in Fig. 8. As follows from this figure, the threshold energy is below 3.5 MeV. However, the signal might be too weak and a gas of higher density might have to be used to increase it.

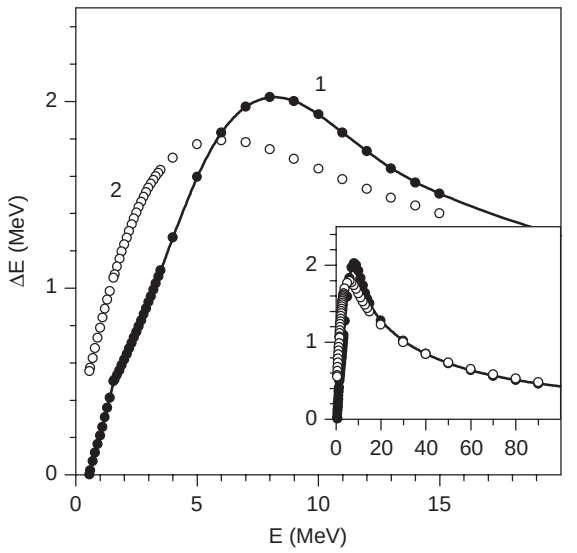

Fig. 8. The calculated energy loss for ^{12}C in the first air gap of the chamber (1) and in the entrance window cathode (2) versus the incident energy.

5. Conclusion

The described multichannel air-ionization chamber is suitable for the monitoring of medical beams and the measurement of their 2D-profile.

The very thin cathode windows and anodes consisting of 1.5-μm polyimide films coated by a 0.2-μm conductive layer which were used as electrodes have allowed us to significantly reduce the beam disturbance.

Moreover, the very low noise as well as the narrow 2-mm gap between the electrodes allowed to achieve a high sensitivity of the chamber. This has been proved in our measurements with a small radioactive β-source and with average proton beam currents from 1 up to 1000 pA.

The signal shape of each pulse was digitized by a multichannel readout electronics system giving us full information about the energy losses in the chamber during irradiation. The shape of the device time response corresponds to the accelerator's macro-pulse.

A dose-depth distribution with a typical Bragg peak was measured.

No ageing effects were observed for about 10^{17} protons passing through the chambers during two accelerator runs in April and in December 2003.

All these advantages make it promising to use the device in radiotherapy with protons as well as with other particles. A chamber filled with a dense gas can also be used as a tracking detector for nuclei at low energy.

Acknowledgements

We thank the staff of the INR Experimental Complex Department for assistance during the accelerator runs.

References

[1] F. Pedrony, et al., Med. Phys. 22 (1995) 37.
[2] J.H. Timmer, et al., Nucl. Instr. and Meth. A 478 (2002) 98.
[3] C. Brucasco, et al., Nucl. Instr. and Meth. B 168 (2000) 578.
[4] C. Brucasco, et al., Nucl. Instr. and Meth. A 389 (1997) 499.